Investigation of under-expanded jet screech associated convective velocity based on high frequency sampled schlieren visualisations

Bertrand Mercier, Thomas Castelain, Christophe Bailly

Investigation of under-expanded jet screech associated convective velocity based on high frequency sampled schlieren visualisations

B. MERCIER[a] , T. CASTELAIN[b] , C. BAILLY[c]

a. Ph.D. Student, Université de Lyon, Laboratoire de Mécanique des Fluides et d'Acoustique, UMR CNRS 5509, 36 Avenue Guy de Collongue ; bertrand.mercier@doctorant-ec-lyon.fr.

b. Assistant Professor, Université Lyon 1, 43 Boulevard du 11 Novembre 1918, 69622 Villeurbanne Cedex ; Laboratoire de Mécanique des Fluides et d'Acoustique, UMR CNRS 5509. thomas.castelain@ec-lyon.fr

c. Professor, Université de Lyon, Laboratoire de Mécanique des Fluides et d'Acoustique, UMR CNRS 5509, 36 Avenue Guy de Collongue. christophe.bailly@ec-lyon.fr ...

Résumé :

L'étude concerne l'analyse des données mesurées à partir d'un dispositif de visualisation schlieren, sur un jet supersonique rond sous-détendu à M_j=1,15. L'acquisition de séquences de plusieurs centaines de milliers d'images schlieren consécutives à la fréquence de 430 kHz permet des analyses originales des phénomènes associés au screech. Deux méthodes de traitement sont développées et font apparaître les caractéristiques d'une onde stationnaire produite par l'interaction entre le champ de densité aérodynamique des grandes structures turbulentes descendant l'écoulement et le champ acoustique remontant le jet. L'analyse de l'onde stationnaire permet l'étude de la vitesse de convection des structures. Les résultats indiquent une vitesse de convection dépendante de la position axiale dans le jet, qui remet en cause les modèles simples de prédiction de la fréquence du screech.

Abstract :

The present study is based on schlieren visualisations constituted by hundreds of thousands frames filmed at a frame rate of 430 kHz of a screeching circular under-expanded jet operated at M_j=1.15. Two processing methods are introduced and point out a standing wave pattern. The features of this standing wave are used for the estimation of coherent structures convective velocity. It is found that convective velocity is varying along the jet, which is not consistent with commonly used screech frequency prediction models.

Key words : Jet, Screech, Convective velocity, Standing wave, Schlieren

1 Introduction

In this work is considered the tonal component of acoustic spectrum emerging from under-expended jet. This tone is referred to as screech since its first description by Powell [1]. The screech mechanism is explained by Powell as a four stages sequence : instability waves grow in mixing layer and are convected downstream, they interact with shocks involving acoustic radiations, then acoustic propagates upstream, and finally the acoustic wave interacts with the mixing layer in the near nozzle region. This interaction initiates a new instability wave so the process is self-maintained. In order to keep the upstream propagating acoustic waves generated by different shocks coherent, Powell expressed the phase criterion which lay in the principle that the coherent structures travelling time to reach a shock in addition to the time spent by the acoustic wave to return to the nozzle must be a integer multiple of the screech period [1]. The screech period T_s is then given by

$$T_s = \frac{L_s}{U_c} + \frac{L_s}{C_0} \tag{1}$$

where L_s is the shock cell length, U_c is the convective velocity of screech associated coherent structures and C_0 is the speed of sound in the surrounding medium. Letting M_c be the convective Mach number relative to C_0, one can derive from equation (1) the screech frequency f_s in the commonly used form :

$$f_s = \frac{U_c}{L_s\,(1 - M_c)} \tag{2}$$

Tam [2] also derived a frequency prediction model known as the weakest link theory and based on the broadband shock associated noise. The Tam's model leads to the same equation as (2).

Westley and Wooley [3] observed in the near field sound pressure a partial standing wave pattern resulting from shock cell associated distributed sources, nozzle flange reflection and convected structure's hydrodynamic pressure field. Later, Panda [4] confirmed that a partial standing wave is observed from RMS near field pressure measurements, and cross-spectra within the shear layer. Consequently Panda proposed the screech frequency to be dependent on the partial standing wave length L_{sw} instead of the shock cell length. This turns into the new formulation

$$f_s = \frac{U_c}{L_{sw}\,(1 - M_c)} \tag{3}$$

Note that L_{sw} and L_s are similar in magnitude, for instance with the M_j =1.15 jet which is considered for the present study, L_s is found about 10% higher than L_{sw}.
Yet, these two formulations are consistent in terms of numerical values, they emerge from two different concepts. Powell's and Tam's models are both theories involving the physical process based on the acoustic feedback induced by shock/structure interactions. Panda's model rely on the observation of a standing wave which might be related to screech frequency using equation (3) assuming interaction between two waves, but the acoustic sources are not considered.

The main purpose of the present study is to investigate the screech feedback loop in order to confront the previously quoted models with experimental results and to discuss their respective validity.

2 Experimental set-up

Data presented in this work are measured in the supersonic wind tunnel exhausting in the anechoic chamber of the Laboratoire de Mécanique des Fluides et d'Acoustique at École Centrale de Lyon. The supersonic jet is under-expanded, thus characterized by a shock-cell structure, and flows from a 38mm diameter convergent nozzle which is detailed by André *et al.* [5]. The jet is characterised by its nozzle pressure ratio (NPR) defined as the ratio of plenum pressure to ambient pressure. A given NPR corresponds to a given equivalent perfectly expanded jet Mach number M_j assuming isotropic flow across the nozzle outlet. This study focuses on jet operated at a $NPR = 2.27$ - $M_j = 1.15$, but it can be noted that results presented here after are tested for other NPR of slightly under-expanded jet with same conclusions.

Experimental data are acquired from a conventional Z schlieren apparatus with knife edge perpendicular to the jet axis which reveals axial density gradient in the flow. For measurements, a Phantom V12 camera was used at 430769 Hz sampling rate allowing an exposure time of 2.3 μs and 640*16 pixels in frames. The sampling time is about 1.2s. Each pixel is 0.261mm width (about 145 pixels per nozzle diameter) in the jet plane. The field of vision is delimited by $y/D = 0.42$ to 0.56 in radial direction and $x/D = -0.1$ to 4.2 in axial direction, thus the nozzle lip line is within this range which allows shear layer investigation. Further details of the experimental conditions are fully described in André *et al.* [5, 6]. The combination of the high sampling rate, the fine resolution and the large amount of sample (about 520000 frames per record) rises this measurement apparatus above most of systems used for previous studies in terms of post-processing possibilities and flow features content. One disadvantage of this method is the difficulty to obtain absolute quantitative values. No attempt of calibration or deconvolution correction has been applied, hence data presented consist in analyses of the raw images and are then presented in arbitrary units (gray level).

3 Convective velocity extraction

3.1 Post-processing methods

For the purpose of this study two post-processing methods are presented. The first is discussed in this section and deals with the extraction of the convective velocity from schlieren visualisations. In this way, time histories of gray levels gathered from pixels of the studied region are first extracted from schlieren films. The chosen region is a line at constant $y/D = 0.5$ (y is pointing toward radial direction) along which screech associated structures are expected to travel. In order to split broadband turbulent structures from screech associated turbulent structures, a band pass IIR filter is applied in time domain on all extracted pixel's signals. The center frequency of the filter is set at screech frequency and cut-off frequency are arbitrary set at $\pm 5\%$ of center frequency. The narrow band is necessary to obtain a suitable signal to noise ratio but, if too much narrow, eventual variations of screech frequency in time might be filtered out. issues involved by phase lag and group delay are avoided by using zero-lag filtering consisting of a causal followed by a non-causal application. Since each pixel associated time history is filtered and since the filtering process is applied in phase for all pixels, the signal along the lip line ($y/D = 0.5$) can be rebuilt at every sample times. An illustration of the results is provided in the animated figure 1 for one screech period chosen randomly within the thousands contained in the record. The dashed line represents the envelope. The upper one is defined as to be the signal maxima

recorded during the studied period for every location along the considered line. The lower one is same but according to minima. This envelope contains some noise disturbing the automatic processing the which is filtered by a low pass filter as described in the next section. A major characteristic of the envelope is the spatial modulation of the amplitude. The wavelength of the modulation is found to be smaller than the shock cell length. For instance, the mean wavelength of the modulation over the range of x/D between 1 to 4 is $0.60D$ whereas the mean shock cell length of the six first cells is 0.67D. This result was observed by Panda [4] who related it with Westley and Wooley [3] observation as a so called standing wave. Since this modulation is most probably corresponding to the standing wave effect and its wavelength L_{sw} can be measured, it is possible from equation (3) to derive the following expression for U_c :

$$U_c = \left(\frac{1}{C_0} - \frac{1}{f_s L_{sw}} \right)^{-1} \tag{4}$$

3.2 Results

The method presented in this section reveals original characteristics in that sense that no hypothesis is needed about the stationary state of the process. Each period can be studied independently. The easiest observable time dependent quantity is the intensity of screech and so the amplitude of modulation, nevertheless the amplitude must be high to ensure a good signal to noise ratio which is essential for accurate processing. Periods for which screech activity is too low with respect to an arbitrary limit are thus rejected from the data to be processed.

The convective velocity extraction rests upon equation (4) that relates the envelope modulation wavelength L_{sw} to the convective velocity U_c. L_{sw} is measured from the envelope as the distance between two maxima or two minima. However the envelope of the raw signal contains some noise emerging from the noise in the signal shown in figure 1. This affects the extrema detection process and envelope must therefore be zero lag filtered by a low pass second order IIR filter that cut above 20% of the wave-number calculated with $U_c = 0.65U_j$. Note that some care is taken to remove the bias in wavelength estimation introduced by the low wave number modulation expressing instability wave growth and decay. This leads to the clusters of U_c represented in figure 2. One can notice that clusters are fairly aggregated before x/D of about 2 and become more scattered after. This transition also correspond to the change in growth rate sign. Some estimated convective velocity stand at about $U_c/U_j = 0.3$. Their presence is explained by the limit of the low-pass filter efficiency that some times allow a local extrema to exist, for instance due to the presence of a shock in the near field. This extrema is then used for wave length measurement which leads to errors in convective velocity. It is primarily those kind of bias that are avoided by processing only periods corresponding to highest signal to noise ratios. After cleaning clusters from biased data, the average velocity is shown in figure 6 by diamond markers and error bar given at plus or minus two standard deviations.

The convective velocity is first increasing with downstream distance from $0.4U_j$ to $0.68U_j$ up to x/D of about 3 and starts decreasing further downstream. $U_c = 0.68U_j$ is a value commonly used is the Powell's or Tam's model for prediction of slightly under-expended jet screech frequencies, however this velocity is generally assumed to be constant. Yet, neither the convective velocity as slow as $0.4U_j$ or its spatial dependency have been related so far.

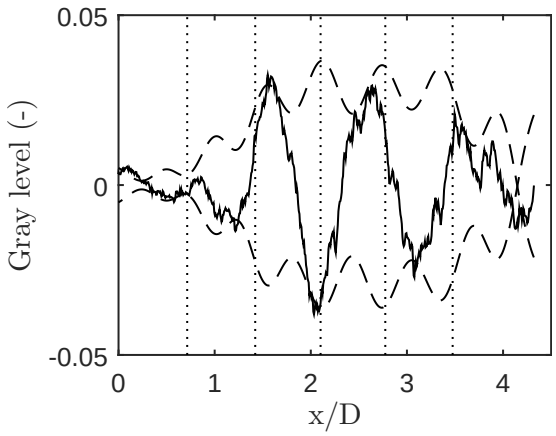

FIGURE 1 – —, Signal obtained from time filtering method for $M_j = 1.15$ at the lip line. - - -, Envelope associated with the filtered signal (Animated figure over one period).

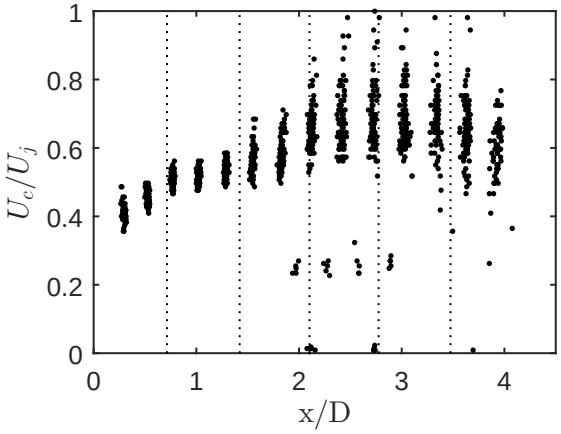

FIGURE 2 – Scatter plot of all the estimations of convective velocity normalized by U_j at M_j=1.15 along the lip line.

4 Phase velocity extraction

4.1 Post processing method

The phase velocity is studied through a phase averaging process. It consists in sorting and averaging images according to their phases with respect to screech cycle. This method requires a reference signal from which phase is known. This signal must present a high signal to noise ratio to ensure accuracy in phase, so it is determined by using the time history of the gray level associated with a pixel located in a quiescent region upon the nozzle where acoustic prevails over hydrodynamic. After band passing the reference signal around screech frequency, each local maximum corresponding time t_i is recorded in a table. From t_i is defined the period as $T_i = t_{i+1} - t_i$, and finally each frame phase ϕ is estimated as follows :

$$t \in [t_i; t_{i+1}], \quad \phi = 2\pi \frac{t - t_i}{T_i} \tag{5}$$

Updating the screech period every screech cycle allows some variations of screech frequency in time without loss of coherence after averaging which cannot be performed under constant frequency assumption. For the sake of convenience in phase velocity extraction, phase is estimated over three periods. Assuming the period is constant over this short range, equation (5) is finally treated as :

$$t \in [t_i; t_{i+3}], \quad \phi = 2\pi \frac{t - t_i}{3T_i} \tag{6}$$

4.2 Results

An example of results is provided in figure 3 for a screech period by increment in phase of $\pi/4$. Since the corresponding phase of all frames is estimated from equation (6) raw images can be sorted in bins of constant phase-width, and the resulting phase-averaged images can be processed by averaging all images

contained in each bin. Processed images are then composed by the average of broadband turbulence in addition to screech associated coherent structures. The average part is removed by subtraction of the mean image based on the full record, so only the screech associated signal remains.

The animated figure 4 presents the result of time averaged method with a resolution of 4° over only one screech period of the three computed from equation (6). This figure looks similar to figure 1 but expresses an averaged process so the study of time dependent quantities such as screech amplitude is not relevant. However it allows a rather high signal to noise ratio so filtering associated issues are minimized. Same features as with time filtering in terms of envelope modulation are observed.

The phase velocity is computed through the analysis of zero crossing location evolution with phase. They are marked by crosses in figure 4, and those corresponding to raising edge are reported in the $(x/D, \phi)$ plane in figure 5. Figure 4 is therefore composed by curves that correspond to the survey of the associated coherent structures over three periods of screech.

The inverse of the local slope of these curves represents the distance travelled for an increment of phase, thus an increment of time. Therefore the phase velocity is equivalent to the inverse of the slope. Local phase velocity derived from this slope is shown in figure 6 by cross markers and normalised by U_j. The first notable point is the modulation of the velocity, in the order of 50% of the average. This is in phase with the modulation of the envelope and is presumed to be the consequence of the hydrodynamic/acoustic interaction. The same behaviour is noticed by Panda [7] who used both the phase averaged method and two probes cross-spectrum. The second point is the tendency for the phase velocity to increase with downstream distance. This is clear when looking at maxima of the signal or from a different point of view on curves of figure 5 that tend to bend toward lower slope, hence larger velocity. Finally, it is to note that before the first shock, the curve slopes are negative which imply negative phase velocity. This slope is explained by the low level of the hydrodynamic screech associated coherent structures pressure field. In effect at the beginning of the growing process, acoustic pressure level is higher than hydrodynamic pressure level, so the resultant wave moves upstream. When turbulent structures are large enough to offset acoustic, and because propagating velocity are similar, a quasi-standing wave comes out locally and turns into the vertical lines in figure 5 right after the first shock, it is also visible as a fluctuation node in figure 4. The jump between negative and positive slope regions is introduced by the definition of raising edge used for detecting zero crossing, in effect, the raising edge of the negative slope region should be chosen as the falling edge for consistency according to the converse velocity direction. This discontinuities disappear when all zero crossing points are used for the figure.

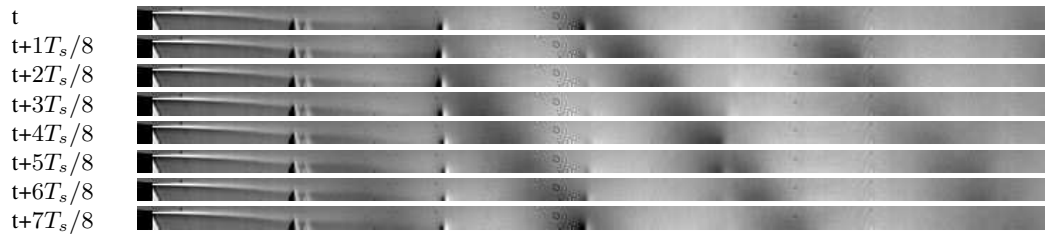

FIGURE 3 – Phase averaged snap shots over a screech period for M_j=1.15. Data obtained from schlieren images

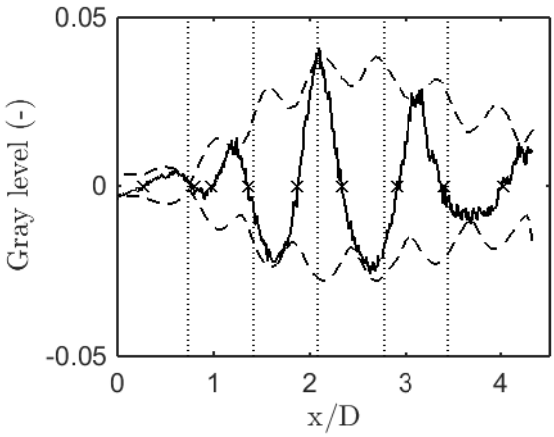

FIGURE 4 – —, Signal obtained from phase averaging method for M_j=1.15 at the lip line. - - -, Envelope associated with the filtered signal (Animated figure over one period).

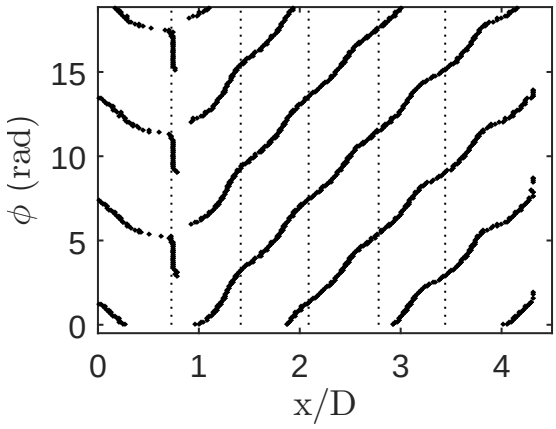

FIGURE 5 – Phase corresponding to locus of raising edge zero crossing over three periods at M_j=1.15.

5 Discussion about Powell's phase criterion

The Powell's phase criterion [1] is a condition for screech amplification that rests upon the necessity for the time spent in a loop, that is convection time plus acoustic feedback time, considering each shock to be an integer multiple of the screech period. In this purpose two assumptions are made and consist in a constant convective velocity and a constant shock cell length.

According to the presented results, the constant convective velocity assumption is questionable. In addition the shock cell length tends to decrease with downstream distance. The effect of these two results leads to the conclusion that the loop time cannot be an integer of screech period for each shock. However, no account is taken of the propagation time across the shear layer. This effect may balance evolution of the two changing parameters to keep the phase criterion valid.

6 Conclusion

Two post processing methods have been applied on high frequency recorded schlieren visualisation of an under-expanded screeching jet at $Mj = 1.15$. These methods produce comparable results that allow investigation of space and time development of the observed signal. Observations of acoustic and hydrodynamic features support the idea already developed by Westley & Wooley [3] and Panda [4] that the signal is the result of summation of convected instabilities and retrograde acoustic waves density gradient fields.

It is noticeable from figure 6 that some care must be taken when studying and interpreting velocities. The convective velocity and the phase velocity of the measured wave are somehow different, even if particular features can be observed on both.

The present study points out the modulation of the phase velocity that was an expected result according to Panda's description of the hydrodynamic/acoustic standing wave. The second result concerns the convective velocity found to be space dependent with a tendency to raise up to a maximum at the fourth shock cell. This spatial dependency questions the Powell's phase criterion and Tam's weakest link theory that both require constant convective velocity.

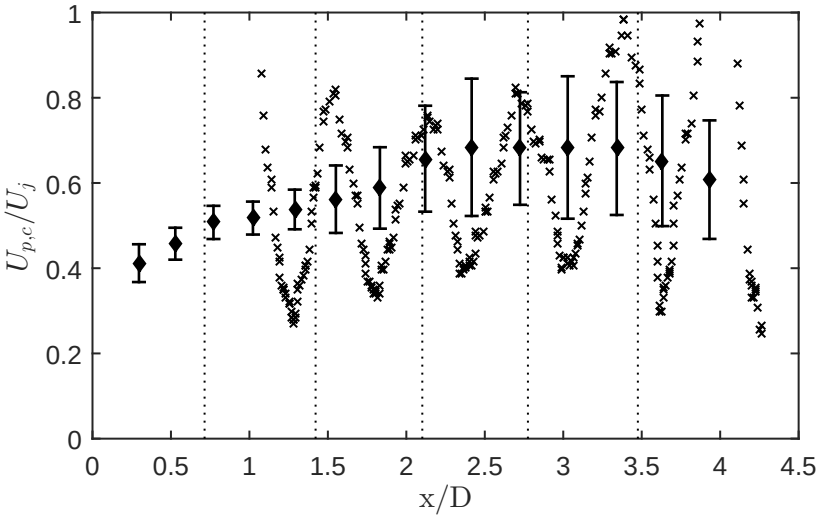

FIGURE 6 – Experimental data of velocities measured at M_j=1.15. $\times$: Phase velocity extracted from the phase averaged method. ♦ : Convective velocity estimated from envelope modulation wave length and averaged for each clusters with the associated ± 2 standard deviation error.

Acknowledgments

This work was performed within the framework of the Labex CeLyA of Université de Lyon, within the program "Investissements d'Avenir" (ANR-10-LABX-0060/ ANR-11-IDEX-0007) operated by the French National Research Agency (ANR). The authors also wish to thank Benoit André for his experimental work that stands this study.

Références

[1] Powell, A. *On the mechanism of choked jet noise*, Proceedings of the Physical Society. Section B, 66(12), 1953

[2] Tam, C.K.W. and Seiner, J. and Yu, J *Proposed relationship between broadband shock associated noise and screech tones*, Journal of Sound and Vibration, 110(2), 1986

[3] Westley, R. and Woolley, JH. *The near field sound pressures of a choked jet during a screech cycle*, AGARD Conference Proceedings, 42, 1969

[4] Panda, J. *An experimental investigation of screech noise generation*, AIAA Paper, 96-1718, 1969

[5] André, B. and Castelain, T. and Bailly, C. *Shock-Tracking Procedure for Studying Screech-Induced Oscillations*, AIAA Journal, 49(7), 2011

[6] André, B. *Étude expérimentale de l'effet du vol sur le bruit de choc de jets supersoniques sous-détendus*, PhD Thesis, Ecole Centrale de Lyon, 2012

[7] Panda, J. and Raman, G. *Underexpanded Screeching Jets From Circular, Rectangular, and Elliptic Nozzles*, AIAA Paper, 97-1623, 1997